Nanostructured Metallic Glasses: Tailoring the Mechanical Properties of Amorphous Metals

T. Brink, O. Adjaoud, K. Albe

published in

NIC Symposium 2016
K. Binder, M. Müller, M. Kremer, A. Schnurpfeil (Editors)

Forschungszentrum Jülich GmbH,
John von Neumann Institute for Computing (NIC),
Schriften des Forschungszentrums Jülich, NIC Series, Vol. 48,
ISBN 978-3-95806-109-5, pp. 191.
http://hdl.handle.net/2128/9842

Nanostructured Metallic Glasses: Tailoring the Mechanical Properties of Amorphous Metals

Tobias Brink, Omar Adjaoud, and Karsten Albe

Fachgebiet Materialmodellierung, Institut für Materialwissenschaft,
Technische Universität Darmstadt, Jovanka-Bontschits-Str. 2, 64287 Darmstadt, Germany
E-mail: {brink, adjaoud, albe}@mm.tu-darmstadt.de

The mechanical properties of metallic glasses cannot only be influenced by their chemical composition, but also by their nanostructure: Secondary phases in the form of precipitates, as well as a nanocrystalline-like structure in the glass are viable options to increase the plasticity of the material. We performed molecular dynamics simulations on Cu-Zr based metallic glass systems to investigate the influence of these nanostructures on the mechanical deformation.

1 Introduction

Metallic glasses (MG) are metastable materials that were first synthesised in 1960 by rapidly quenching an Au-Si alloy from the melt[1]. In 1988, bulk metallic glasses (BMG) with sample thicknesses above 1 mm were realised and have enabled the use of MGs in engineering applications[2]. These materials are usually highly alloyed to improve the glass forming ability, thereby reducing the critical cooling rate and increasing the sample thickness. They have advantageous mechanical properties, foremost their high yield strength and large elastic strain limit. One obstacle for widespread engineering applications is the brittle failure, especially under tension, of MGs at room temperature[2,3]. The origin of this behaviour, shown in Fig. 1(a), is the localisation of the deformation in a single, dominant shear band. Unlike dislocations, which are line defects, shear bands are two-dimensional defects which are softer than the surrounding matrix, leading to shear softening and the aforementioned strain localisation. Fig. 1(b) compares dislocations with shear bands. Similar to crystalline materials, carefully engineered microstructures may offer possibilities to tailor the mechanical properties. If we take inspiration from these materials, we can imagine two main approaches for influencing shear band nucleation and propagation in the glass: (1) Secondary phases in the form of precipitates and (2) a "grain" structure in the glass. The idea behind composites consisting of a MG matrix with crystalline precipitates is illustrated in Fig. 1(c): The crystal phase can either act as an obstacle to shear band propagation or partake in the plastic deformation. It was found experimentally that a large volume fraction of crystalline phases can lead to pronounced plasticity even under tension, for example in Cu-Zr-based MGs[4,5] (for a complete discussion of the relevant literature see Ref. 6). Despite a growing interest in crystal–glass composite materials, our understanding of the interaction between shear bands and precipitates is still incomplete. Recent simulation studies found that crystal–glass interfaces serve as nucleation sites for shear bands[7], but the influence of crystalline precipitates on the propagation of pre-existing shear bands is not understood in detail. To further advance our understanding of composite materials, we investigated this scenario in Cu-Zr based MGs. Contrary to precipitates, which can be grown easily by thermal annealing, a grain structure in amorphous materials

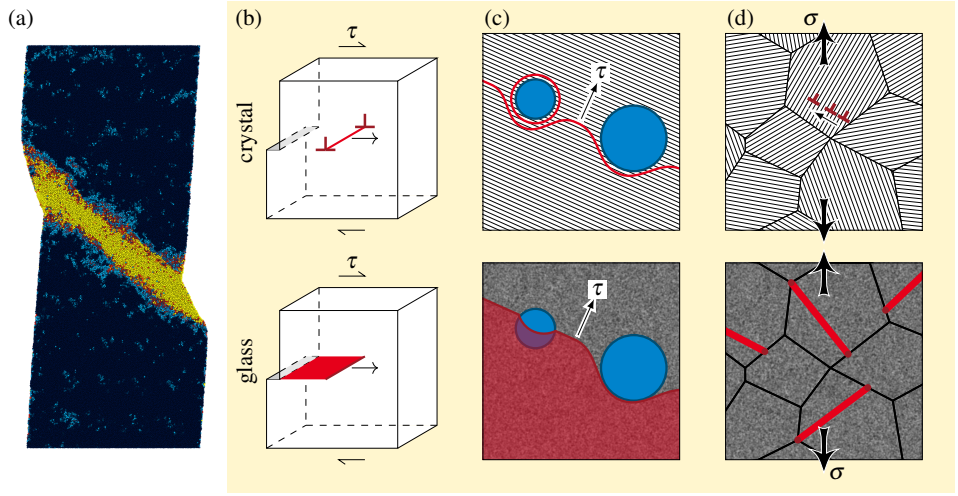

Figure 1. (a) A shear band in a $Cu_{64}Zr_{36}$ MG nanowire. The atoms are coloured according to their atomic strain. (b) Comparison between dislocations in crystals, which are line defects, and shear bands in metallic glasses, which are planar defects. Propagation of the shear band front leaves a mechanically softened region behind (red plane in the bottom picture). (c) Similar to precipitates in crystalline metals, precipitates in MGs may block or influence shear band propagation. (d) Inspired by nanocrystalline metals, nanoglasses consist of glassy grains and exhibit modified mechanical properties.

at first seems implausible due to the lack of a crystal lattice mismatch at the grain boundaries. Still, amorphous nanostructures similar to nanocrystalline samples can be obtained [cf. Fig. 1(d)]. These so-called metallic nanoglasses (NG) consist of amorphous grains connected with glass–glass interfaces and can be produced by cold compaction of glassy nanospheres which are prepared by inert-gas condensation[8]. The resulting interfaces exhibit changes in density and/or composition compared to the bulk[8], as well as a reduced short-range order[9]. $Sc_{75}Fe_{25}$ NGs have been shown to exhibit an excellent plasticity under uniaxial tension relative to BMGs with the same chemical composition[10]. Molecular dynamics simulations demonstrate that the deformation behaviour of NGs can be modified by varying the volume fraction of the glass–glass interfaces[7,11]. Nevertheless, previous structural models obtained with computer simulations are not able to correctly reproduce the density and composition changes observed experimentally. The goal is therefore to find a proper structural model for Cu-Zr based NGs and to investigate the deformation mechanisms of NGs.

2 Computational Methods

To investigate the underlying mechanisms of mechanical deformation, a computational method with atomic resolution, high performance, and scaling to millions of atoms is required. In the current work, we therefore employed molecular dynamics simulations using the software LAMMPS[12]. The interatomic forces were modelled using the Finnis-Sinclair type potential for Cu-Zr by Mendelev *et al.* which provides a realistic description of the

short range order of the MG[13]. Deformations used a strain rate of $4\times10^7/\mathrm{s}$. To stay in a regime of localised deformation despite the high strain rates, the simulations were carried out at a temperature of 50 K[7]. The biggest work packages contained up to 18 million atoms and were run on JUQUEEN using a hybrid OpenMP/MPI scheme with 8 threads $\times$ 4096 processes. We found that LAMMPS efficiently scales to this problem size with only minor losses. The resulting data were analysed and visualised using OVITO[14].

3 Metallic Glasses with Crystalline Nanoprecipitates

We investigated the interaction between an approaching shear band and a crystalline precipitate in order to understand the plasticity in crystal–glass composites[6]. To that end we

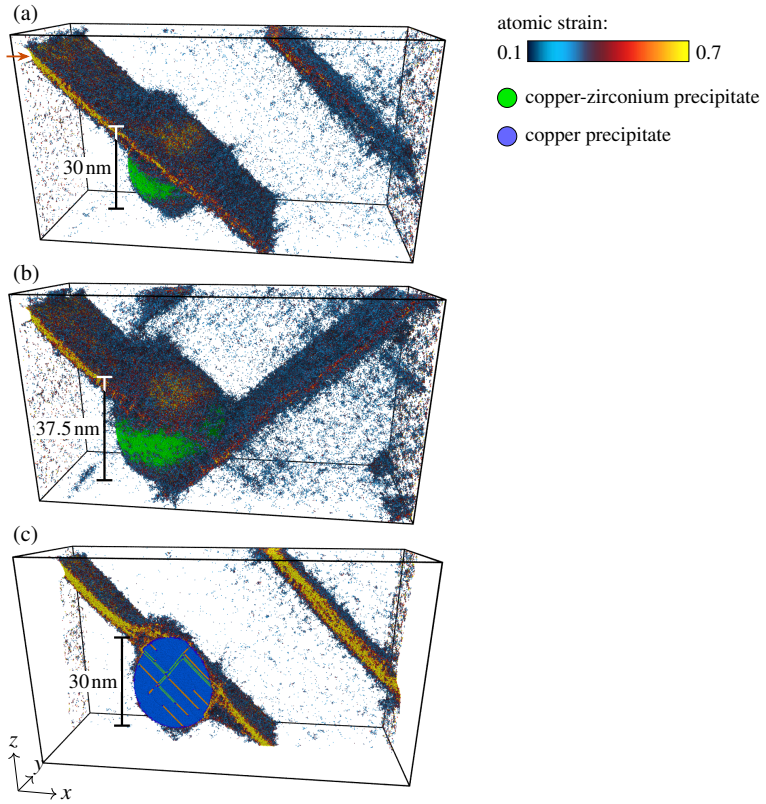

Figure 2. Interaction of shear bands with nanocrystalline precipitates. (a) A shear band originating from the notch on the left (arrow) hits a CuZr precipitate with a diameter of 30 nm. The precipitate does not deform plastically and the shear band simply wraps around the obstacle. (b) If the particle becomes bigger, the wrapping becomes impossible and the shear band is stopped. Due to the remaining stress in the system a new shear band is nucleated immediately perpendicular to the blocked one. (c) By exchanging the crystal phase for a softer one, in this case copper, we can observe slip transfer into precipitate. The snapshot shows a slice through the middle of the precipitate, the orange and green atoms represent stacking faults.

prepared glass samples and inserted precipitates of varying size and with varying distances between them. We used periodic boundary conditions in y and z direction and free surfaces in x direction. To control the origin of the shear band, which would otherwise start from the crystal-glass interface[7] or a random point on the surface, we introduced a notch on the surface. The notch is positioned such that a shear band nucleating from it under tensile deformation in z direction will hit the precipitate. First, we inserted CuZr precipitates, using the experimentally observed B2 crystal structure[15] and performed tensile tests. We observed that these precipitates only deform elastically and therefore simply present an obstacle for the shear band. This may be an artefact of using the Mendelev potential but presents a good model for precipitates with yield stress far above the glass matrix. Precipitates with a size below 25 nm to 35 nm (the exact diameter depends on the distance between the precipitates) do not stop the shear band propagation. Instead, the shear band simply wraps around the obstacle as depicted in Fig. 2(a). In contrast to the case in a crystalline matrix, this change of direction is made possible by the lack of a crystallographic lattice. Increasing the precipitate size above the critical diameter leads to behaviour as shown in Fig. 2(b): The shear band is blocked by the precipitate. The resulting build-up of stress leads to the nucleation of a second shear band at the crystal–glass interface opposite the initial shear band. Usually, shear bands move on planes of highest resolved shear stress. When bypassing an obstacle, the shear band must leave this favourable plane and temporarily move in a plane of lower resolved shear stress. At a critical precipitate size, the resolved shear stress becomes so low that it is more favourable to nucleate a new shear band. In this case shear bands may be temporarily stopped or deflected, but tensile plasticity cannot be achieved: In the end, a dominant shear band will appear and lead to failure shortly after the elastic limit.

Another case that needs to be taken into account, is a crystal phase that allows a slip transfer from the shear band in the matrix into the crystal. As a model, we chose copper precipitates. Due to greatly overestimated unstable stacking fault energies in the Mendelev potential, we switched to a different Cu-Zr potential, which cannot correctly describe CuZr in the B2 structure but reproduces the copper fcc crystal[16,17]. The results of this simulation are presented in Fig. 2(c). Instead of blocking the shear band, the precipitate participates in the plastic deformation: Slip transfer through the particle can be observed. In composites like this, the blocking of the shear band is replaced by the participation of the crystalline phase in the plastic deformation. If the crystalline volume fraction is large enough, the macroscopic mechanical response will be a mixture of both phases. These systems hold the promise of a mix of favourable properties of crystalline metals and MGs.

4 Nanoglasses: Metallic Glasses with Microstructure

4.1 Synthesis and Microstructure

NGs are obtained by compacting a powder of amorphous nanospheres produced by inert-gas condensation[8]. In the inert-gas condensation process, gasses of the constituting elements condense into glassy nanospheres in an inert-gas atmosphere. The spheres are initially of a high temperature, an aspect of the synthesis not taken into account by previous atomistic modelling. To simulate the relaxation of the spheres at high temperature, we first cut a glassy nanosphere with a diameter of 7 nm from a $Cu_{64}Zr_{36}$ BMG. The glassy

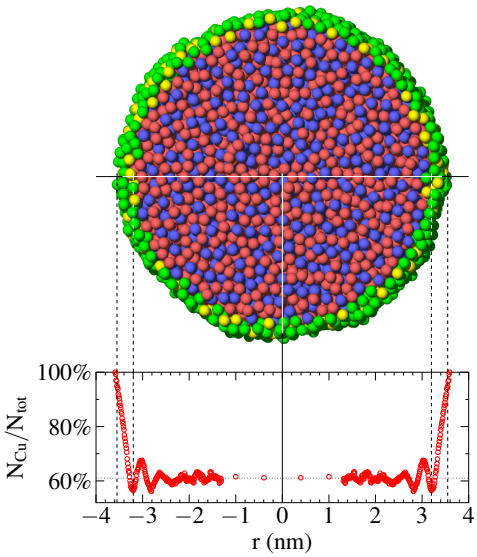

Figure 3. A nanosphere of $Cu_{64}Zr_{36}$ glass. To simulate the conditions of inert-gas condensation, the sphere was annealed slightly above T_g. This leads to a segregation of copper to the surface, where a surface shell with different composition arises. The graph shows a radial scan through the particle, plotting the percentage of copper atoms in the current shell ($N_{\mathrm{Cu}}/N_{\mathrm{tot}}$). The sphere has a radius of 3.5 nm. The surface layer has a width of around 0.3 nm. Red atoms are copper, blue atoms zirconium. In the surface shell, copper is depicted in green and zirconium in yellow.

nanosphere was heated above the glass transition temperature (T_g), held there until equilibrated, and then cooled down to 50 K[18]. We determined the composition variation across the sphere, plotted as a radial profile in Fig. 3. A Cu-rich surface layer with a width of about 0.3 nm is formed. This layer has an average composition of about 72 at.-% copper. Due to the small size of the sphere, the core is slightly copper-depleted, resulting in a composition of $Cu_{61}Zr_{39}$.

We repeated the procedure described above for several glassy nanospheres with diameters ranging from 6 nm to 8 nm to mimic the size variation in the experiment. Fig. 4 portrays the production of a NG from the powder: The differently sized nanospheres are compacted by applying a hydrostatic pressure about 5 GPa[19], comparable to the experimental conditions[8]. As can be seen in Fig. 4(b), the surfaces of the nanospheres turn into interfaces and do not diffuse into the grain interior. The glass–glass interfaces retain their composition of $Cu_{72}Zr_{28}$. These effects, which are due to the surface segregation in the nanospheres, can explain the experimental observation that the interfaces in $Sc_{75}Fe_{25}$ NGs have a different composition than the grain (they are iron-depleted)[8], a phenomenon that was not accounted for in earlier atomistic modelling[7,9,11].

4.2 Plastic Deformation

Using the previously described NG model, we investigated the plastic deformation mechanisms under tension[20]. The engineering stress-strain curve is presented in Fig. 5(b). A

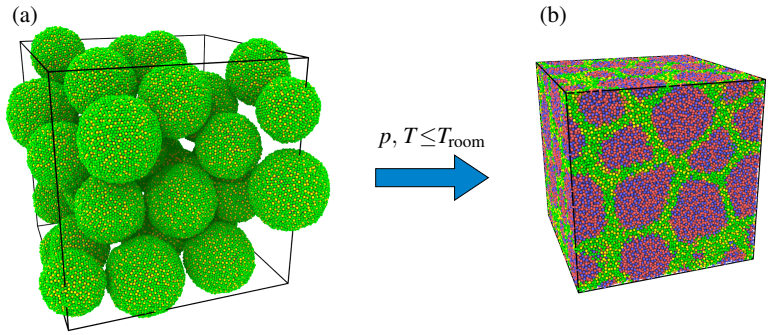

Figure 4. The glass spheres are cold compacted to produce a nanoglass. The surface shell becomes the intergranular interface as evidenced by the colouring of the atoms (same as Fig. 3). This interface retains the changed composition and exhibits a different density compared to the interior of the grain.

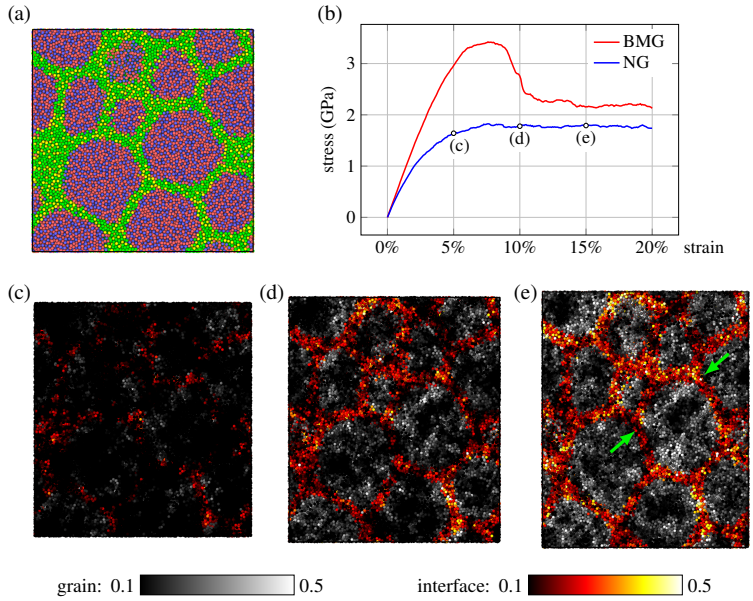

Figure 5. Tensile test of an NG. (a) A slice of the glass before deformation. The stress-strain curve is plotted in (b) together with a stress-strain curve for a bulk metallic glass of the same composition. (c–e) Atomic strain in the slice at 5%, 10%, and 15% macroscopic strain. The deformation almost immediately starts in the interfaces. The grains deform by small shear bands going through them, as indicated by the green arrows. No single shear band has moved through the complete system and become critical, thereby allowing for the finite plasticity of the material.

stress-strain curve of a BMG with the same nominal composition is also shown for comparison. In the case of the BMG, there is a stress drop which is characteristic of the formation of a single shear band, while this stress drop is not observed in the NG. The steady-state

stress remains constant until the end of the simulation at 20% total strain, which indicates that no shear softening is observable. To further get insights into the deformation behaviour at an atomic level, we inspected the atomic strain, which is displayed in Figs. 5(c–e) at 5%, 10%, and 15% macroscopic strain. The deformation starts in the interfaces, which are characterised by a reduced short-range order and therefore reduced strength. At larger strains, shear bands start appearing in the grain interiors due to local stress concentrations induced by grain movement, marked with green arrows in Fig. 5(e). The weakened interfaces also serve as nucleation sources for shear bands. Due to the random 3D arrangement of grains no single shear band becomes dominant, leading to significant plasticity, although at the cost of reduced yield strength. Other simulations already indicate that the grain size also plays a role[11].

5 Conclusion

The mechanical properties of MGs can be tailored via their nanostructure: Both the introduction of secondary phases and of glass–glass interfaces lead to modified shear band nucleation and propagation which influences the plastic deformation as a result. Shear bands can get blocked by precipitates only if the crystal does not deform plastically and is greater than 25 nm to 35 nm. This may lead to the nucleation of new shear bands in lieu of continued propagation of the blocked ones, but cannot prevent the formation of critical shear bands. If the precipitates deform plastically, slip transfer from the shear band into the crystal phase can take place. In these composites, the macroscopic mechanical response is a mixture of both the glass and the crystal phase. NGs are rather new materials that avoid critical shear banding much longer than homogeneous MGs due to their inherent nanostructure. The atomic strain is mostly distributed in the glass–glass interfaces, leading to a more homogeneous deformation. At later stages of the deformation, shear bands appear inside the grains, where they stay localised. These shear bands do not propagate through the sample and therefore do not become critical shear bands.

Acknowledgements

The authors gratefully acknowledge financial support by the Deutsche Forschungsgemeinschaft (DFG) through project grants nos. AL 578/13-1 and AL 578/6-2, as well as the sub-project *Nanoglasses* of SPP 1594 (grant no. AL 578/15). Computing time was granted within the scope of project HDA22 by the John von Neumann Institute for Computing (NIC) and provided on the supercomputer JUROPA at Jülich Supercomputing Centre (JSC), as well as by the Gauss Centre for Supercomputing (GCS) through the NIC on the GCS share of the supercomputer JUQUEEN at JSC.

References

1. W. Klement, R. H. Willens, and P. Duwez, *Non-crystalline structure in solidified gold-silicon alloys*, Nature, **187**, 869–870, 1960.
2. A. Inoue, *Stabilization of metallic supercooled liquid and bulk amorphous alloys*, Acta Mater., **48**, 279–306, 2000.

3. M. F. Ashby and A. L. Greer, *Metallic glasses as structural materials*, Scr. Mater., **54**, 321–326, 2006.
4. Z. Liu, R. Li, G. Liu, K. Song, S. Pauly, T. Zhang, and J. Eckert, *Pronounced ductility in CuZrAl ternary bulk metallic glass composites with optimized microstructure through melt adjustment*, AIP Adv., **2**, 032176, 2012.
5. F.-F. Wu, K. C. Chan, S.-T. Li, and G. Wang, *Stabilized shear banding of ZrCu-based metallic glass composites under tensile loading*, J. Mater. Sci., **49**, 2164–2170, 2014.
6. T. Brink, M. Peterlechner, H. Rösner, K. Albe, and G. Wilde, *Influence of Crystalline Nanoprecipitates on Shear Band Propagation in Cu-Zr Based Metallic Glasses*, Phys. Rev. Appl., submitted, 2015, arXiv:1505.00723 [cond-mat.mtrl-sci].
7. K. Albe, Y. Ritter, and D. Şopu, *Enhancing the plasticity of metallic glasses: Shear band formation, nanocomposites and nanoglasses investigated by molecular dynamics simulations*, Mech. Mater., **67**, 94–103, 2013.
8. J. X. Fang, U. Vainio, W. Puff, R. Würschum, X. L. Wang, D. Wang, M. Ghafari, F. Jiang, J. Sun, H. Hahn, and H. Gleiter, *Atomic structure and structural stability of $Sc_{75}Fe_{25}$ nanoglasses*, Nano Lett., **12**, 458–463, 2012.
9. Y. Ritter, D. Şopu, H. Gleiter, and K. Albe, *Structure, stability and mechanical properties of internal interfaces in $Cu_{64}Zr_{36}$ nanoglasses studied by MD simulations*, Acta Mater., **59**, 6588–6593, 2011.
10. X. L. Wang, F. Jiang, H. Hahn, J. Li, H. Gleiter, J. Sun, and J. X. Fang, *Plasticity of a scandium-based nanoglass*, Scr. Mater., **98**, 40–43, 2015.
11. D. Şopu and K. Albe, *Influence of grain size and composition, topology and excess free volume on the deformation behavior of Cu–Zr nanoglasses*, Beilstein J. Nanotechnol., **6**, 537–545, 2015.
12. S. Plimpton, *Fast parallel algorithms for short-range molecular dynamics*, J. Comp. Phys., **117**, 1–19, 1995, `http://lammps.sandia.gov/`.
13. M. I. Mendelev, M. J. Kramer, R. T. Ott, D. J. Sordelet, D. Yagodin, and P. Popel, *Development of suitable interatomic potentials for simulation of liquid and amorphous Cu–Zr alloys*, Philos. Mag., **89**, 967–987, 2009.
14. A. Stukowski, *Visualization and analysis of atomistic simulation data with OVITO – the Open Visualization Tool*, Model. Simul. Mater. Sci. Eng., **18**, 015012, 2010, `http://ovito.org/`.
15. S. Pauly, J. Das, C. Duhamel, and J. Eckert, *Martensite formation in a ductile $Cu_{47.5}Zr_{47.5}Al_5$ bulk metallic glass composite*, Adv. Eng. Mater., **9**, 487–491, 2007.
16. X. W. Zhou, R. A. Johnson, and H. N. G. Wadley, *Misfit-energy-increasing dislocations in vapor-deposited CoFe/NiFe multilayers*, Phys. Rev. B, **69**, 144113, 2004.
17. L. Ward, A. Agrawal, K. M. Flores, and W. Windl, *Rapid production of accurate embedded-atom method potentials for metal alloys*, arXiv:1209.0619 [cond-mat.mtrl-sci], 2012.
18. O. Adjaoud and K. Albe, *On the origin of compositional gradients in metallic nanoglasses*, in preparation, 2015.
19. O. Adjaoud and K. Albe, *Molecular dynamics simulations of sintering processes of nanometer-sized metallic glassy spheres*, in preparation, 2015.
20. O. Adjaoud and K. Albe, *On the origin of plasticity in metallic nanoglasses*, in preparation, 2015.